JACS
JOURNAL OF THE AMERICAN CHEMICAL SOCIETY
Article
pubs.acs.org/JACS

An Activatable Prodrug for the Treatment of Metastatic Tumors

Eun-Joong Kim,[†] Sankarprasad Bhuniya,[†,∥] Hyunseung Lee,[†] Hyun Min Kim,[†] Chaejoon Cheong,[†,‡] Sukhendu Maiti,[*,§] Kwan Soo Hong,[*,†,‡] and Jong Seung Kim[*,§]

[†]Division of MR Research, Korea Basic Science Institute, Cheongju 363-883, Korea
[‡]Department of Bio-analytical Science, University of Science & Technology, Daejeon 305-350, Korea
[§]Department of Chemistry, Korea University, Seoul 136-701, Korea

Supporting Information

ABSTRACT: Metastatic cancers have historically been difficult to treat. However, metastatic tumors have been found to have high levels of reactive oxygen species such as hydrogen peroxide (H_2O_2), supporting the hypothesis that a prodrug could be activated by intracellular H_2O_2 and lead to a potential antimetastatic therapy. In this study, prodrug **7** was designed to be activated by H_2O_2-mediated boronate oxidation, resulting in activation of the fluorophore for detection and release of the therapeutic agent, SN-38. Drug release from prodrug **7** was investigated by monitoring fluorescence after addition of H_2O_2 to the cancer cells. Prodrug **7** activated by H_2O_2, selectively inhibited tumor cell growth. Furthermore, intratracheally administered prodrug **7** showed effective antitumor activity in a mouse model of metastatic lung disease. Thus, this H_2O_2-responsive prodrug has therapeutic potential as a novel treatment for metastatic cancer via cellular imaging with fluorescence as well as selective release of the anticancer drug, SN-38.

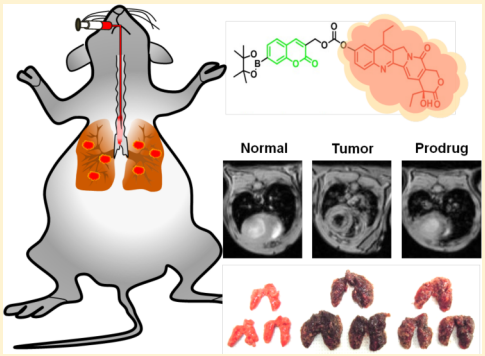

INTRODUCTION

Cancer is one of the most common life-threatening diseases in the world, and metastasis is one of the primary causes of cancer-related death. Although various approaches for cancer therapy have been developed, several barriers to improving effectiveness and avoiding toxicity still remain.[1] In general, cancer cells arise from the genetic transformation of normal cells that allow them to migrate and invade neighboring tissues or distant organs.

In addition, a higher level of oxidative stress has been observed in various cancer cells and tumors due to the overproduction of reactive oxygen species (ROS) including hydrogen peroxide, hydroxyl radical, and superoxide anion.[2] ROS-induced oxidative stress plays a significant role in several pathological processes during cancer progression, such as metastasis, apoptosis, proliferation, and angiogenesis.[3] The excess production of ROS inside cells is closely related to metastatic disease progression, through increased metastatic potential due to the loss of mitochondrial genome integrity.[4] In addition, the intrinsic enhancement of H_2O_2 levels inside the tumor cell induces the expression of metastasis-related growth factors, resulting in invasion and migration.[5]

Taking advantage of these biological features of cancer cells, several approaches have been employed to detect various ROS.[6] Fluorescent probes are an attractive choice for monitoring H_2O_2.[7] Fluorometry is rapidly performed, and can afford real-time information on the localization and quantity of the targets of interest. Therefore, fluorogenic methods have been recognized as a reliable approach for the detection of ROS through the preparation of appropriate probes, suitable linkers, or advanced drug delivery systems.[8]

Theranostic nanomedicine is an emerging technology in biomedicine, which can serve the dual purposes of therapy and diagnosis. Moreover, theranostic approaches are particularly appealing for personalized medicine to improve cancer diagnosis and therapy.[9] With the use of this concept, several types of theranostic prodrug systems have been developed that include anticancer drugs, fluorophores, and guiding groups with thiol responsive linkers.[10]

In synthetic organic chemistry, hydrogen peroxide is neutral, a good nucleophile and can used as a two-electron electrophilic oxidant.[11] Moreover, it is well established that alkyl- or aryl boronic acid and their esters can be easily dissociated by H_2O_2 and the products of this reaction with H_2O_2 and boric acid do not show any cytotoxicity, suggesting that the reaction between boronate moiety and H_2O_2 is chemospecific, bioorthogonal and biocompatible.[12] Therefore, H_2O_2 has drawn great deal of attention as a target for the development of ROS-activated anticancer prodrugs due to their high sensitivity and specificity toward the boronate moiety. Although, some drug delivery systems responsive to H_2O_2 have been reported for cancer treatment, they are lacking a diagnostic component.[13]

In this study, an H_2O_2-activated theranostic agent, prodrug **7**, was developed where a boronate ester was used as a trigger unit, and a coumarin unit was used as a fluorophore to monitor

Received: July 30, 2014
Published: September 11, 2014

   dx.doi.org/10.1021/ja5077684 | J. Am. Chem. Soc. 2014, 136, 13888−13894

the release of SN-38, the chemotherapeutic component. SN-38 is an effective anticancer drug, which is a camptothecin (CPT) derivative. SN-38 is the active metabolite of irinotecan, which is used for the treatment of various types of carcinoma via the inhibition of topoisomerase I.[14] This novel prodrug platform represents the potential for efficient drug delivery into cancer cells with a concomitant increase in anticancer activity, and enhanced fluorescence intensity after boronate ester cleavage triggered by intracellular H_2O_2. The potential *in vivo* therapeutic efficacy of prodrug 7 was evaluated against a mouse metastatic lung tumor model.

RESULTS AND DISCUSSION

Prodrug 7 was synthesized according to the following synthetic pathway as shown in Scheme 1. Compounds **1**−**4** were

Scheme 1. Synthetic Scheme of Prodrug 7 and Reference Compound 8

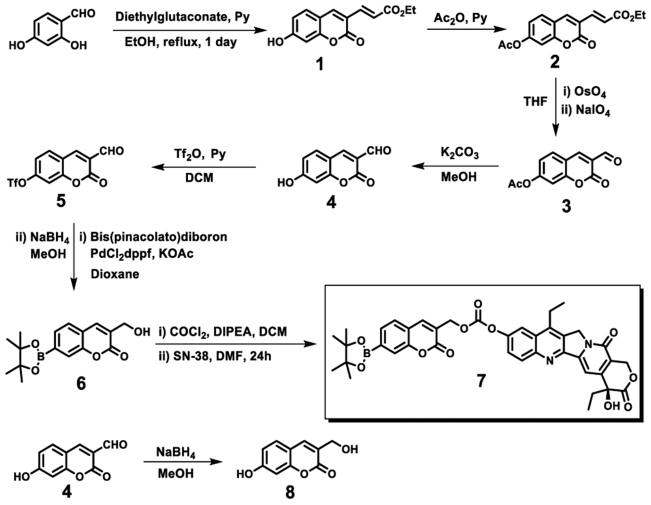

synthesized by previously published methods.[15] Compound **5** was prepared by reaction of **4** with the trifluoromethanesulfonic anhydride in the presence of few drops of pyridine. Compound **5** was reacted with bis(pinacolato)diboron in the presence of catalyst $Pd(dppf)Cl_2{\cdot}CH_2Cl_2$ and KOAc to afford crude boronate-aldehyde coumarin unit, which was reduced by $NaBH_4$ to obtain **6**. Compound **6** was reacted with phosgene, diisopropylethylamine (DIPEA) to give a reactive intermediate, which was successively reacted with SN-38 to yield the desired compound, prodrug 7. The coumarin derivative **8** was used as a reference compound and was synthesized from **4** by $NaBH_4$ reduction. Detailed synthetic procedures, yields and spectroscopic data including ^1H NMR, ^{13}C NMR, ESI-MS, HR-MS are provided in the Supporting Information.

To verify that H_2O_2 was able to convert the boronate moiety to the hydroxyl group in prodrug 7 and consequently activate the coumarin fluorophore, a chemical transformation experiment of prodrug 7 was performed in the presence of H_2O_2 under physiological conditions and monitored by UV−vis and fluorescence spectroscopy. These experiments could verify the H_2O_2-activated drug release mediated by the boronate trigger in cells. In the UV spectrum as shown in Supporting Information Figure S2a, prodrug 7 showed a strong absorption peak at λ_{max} = 320 nm. The absorption peak showed a slight red shift after addition of 300 μm H_2O_2. As shown in Figure 1a, prodrug 7 exhibited weak fluorescence centered at 453 nm,

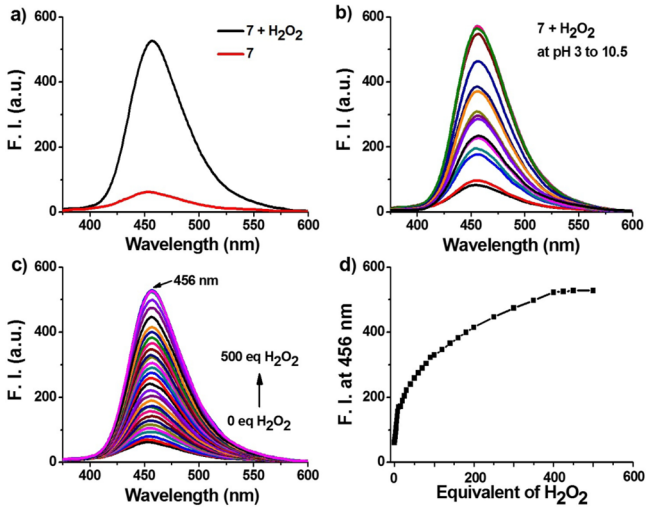

Figure 1. (a) Fluorescence spectra of prodrug 7 (5.0 μM, 10% DMSO, 90% PBS buffer) recorded in the presence and absence of H_2O_2 (300.0 μM). (b) The fluorescence response of prodrug 7 (5.0 μM) with H_2O_2 (300.0 μM) as a function of pH. (c) Fluorescence changes of prodrug 7 (5.0 μM) after treatment with increasing concentrations of H_2O_2 (0−500 equiv). (d) Changes in fluorescence intensity at 456 nm as a function of H_2O_2 concentration.

which increased in intensity about 8.3-fold with a slight red shift upon treatment of H_2O_2 (300 μM) in PBS buffer (10% DMSO). The fluorescence spectra of the solution prodrug 7 after addition of H_2O_2 was exactly the same as the emission spectrum of reference compound **8** (Supporting Information Figure S1).

Furthermore, gradual addition of H_2O_2 up to 0−500 equiv to a solution of prodrug 7 was investigated. The fluorescence intensity of prodrug 7 at λ_{max} = 456 nm increased until it reached a saturation point at 400 equiv H_2O_2 (Figure 1c,d). This observation indicates that the boronate moiety of prodrug 7 was readily dissociated by H_2O_2. Therefore, this ROS in cancer cells might lead to delivery of SN-38 in a dose-dependent manner.

Another set of experiments were performed to determine the role of pH on triggering the release of SN-38 or the fluorophore by monitoring the fluorescence of prodrug 7 (5.0 μM). In the absence of H_2O_2, prodrug 7 is stable over a pH range from 3 to 10.5, as shown in Supporting Information Figure S2b. In the presence of H_2O_2, an enhancement of fluorescence intensity was detected over pH values ranging from 5 to 8, as shown in Figure 1b. These findings showed that a boronate-linked coumarin/SN38 conjugate (prodrug 7) may be useful as a theranostic agent for delivering SN-38 to cancer cells at biological pH.

Efficient release of the active drug from the prodrug is crucial for effective administration of the active drug.[16] To determine the release of active drug over time, fluorescence at λ_{max} = 456 nm was monitored in the presence of different concentrations of H_2O_2 (Supporting Information Figure S4a). The initial rates of fluorescence intensities with time were linearly dependent on H_2O_2 concentration, and it was 123.9 min^{-1} at 400 μmol H_2O_2 as shown in Supporting Information Figure S4b. In the presence of 500 μmol H_2O_2, fluorescence intensity of prodrug 7 reached its highest point and plateaued within 10 min. The kinetics of drug release were faster with 500 μmol H_2O_2 than with 400, 200, or 50 μmol H_2O_2. In contrast, without H_2O_2,

dx.doi.org/10.1021/ja5077684 | J. Am. Chem. Soc. 2014, 136, 13888−13894

there was no fluorescence signal of prodrug 7 at 476 nm as a function of time. This study showed that after prodrug 7 entered the cells, the active drug, SN-38, was released and on the fluorophore activated in less than 10 min.

Before *in vitro* testing, the selectivity of prodrug 7 for H_2O_2 over other biologically relevant ROS species was evaluated. To assess the possibility of interference, prodrug 7 was reacted with various ROS: hydroxyl radical, *tert*-butoxy radical, super oxide, hypochlorite anion, and *tert*-butyl hydrogen peroxide. These ROS were tested under the same reaction conditions as H_2O_2 and fluoresecence was monitored. As seen in Supporting Information Figure S3, increased fluorescence intensity was observed when prodrug 7 was reacted with H_2O_2. No signifiant changes in fluorescence intensity were observed upon addition of other ROS. These findings indicate that prodrug 7 could be reacted selectively with H_2O_2 in the cellular milieu.

In another set of experiments, whether the fluorescence enhancement of prodrug 7 as shown in Figure 1 was an indication of SN-38 release from the prodrug was investigated. Prodrug 7 was reacted with H_2O_2 (300 μM) at 37 °C for 1 h, then an aliquot was subjected to fast atom bombardment mass spectroscopy. From the mass spectra, we observed two main molecular peaks corresponding to reference compound **8** ([M + H] = 193.05) and SN-38 ([M + H] = 393.20) as seen in Supporting Information Figure S27. The MS analyses provided further support for the hypothesis that the boronate moiety present in prodrug 7 was readily cleaved by cellular H_2O_2. The boronate moiety of prodrug 7 reacted as an electrophile with the H_2O_2 nucleophile in a reversible manner to form a negatively charged tetrahedral boronate complex. The C−B bond of this tetrahedral complex then reacted as a nucleophile and to remove the OH group. The rate of reaction between the boronate moiety and H_2O_2 was much faster among other alkyl or aryl peroxides because water is the byproduct and a better leaving group than alcohols. This gives selectivity toward free H_2O_2 over lipid-derived peroxides.[6a] The above investigations suggest that the boronate moiety present in prodrug 7 could be cleaved by H_2O_2 releasing the active drug, SN-38, along with the fluorescent probe **8**, in the cellular milieu as described in Scheme 2. This type of boronate oxidation by H_2O_2 could readily be applied to create a number of tumor-targeting drug conjugates that could be effective in biological systems.

Scheme 2. Proposed Reaction Mechanism of Prodrug 7 with H_2O_2 under Physiological Conditions

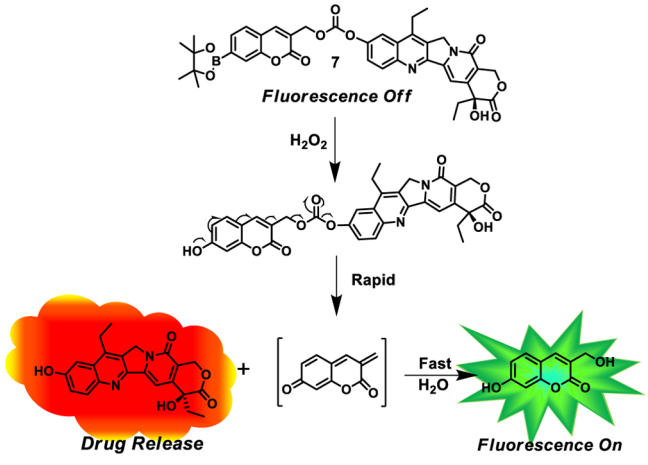

On the basis of the positive results showing H_2O_2-mediated release of active drug and concurrent fluorescence activation, prodrug 7 was tested in cultured cells. Cellular uptake and enhanced fluorescence intensity of prodrug 7 were investigated in two different cell lines, B16F10, a highly metastatic murine melanoma, and HeLa, human cervical cancer cell line.

To determine whether the active form of prodrug 7 induces the fluorescence activation, fluorescence imaging of tumor cells was used to estimate free coumarin formation as shown in Figure 2 and Supporting Information Figure S5. B16F10 and

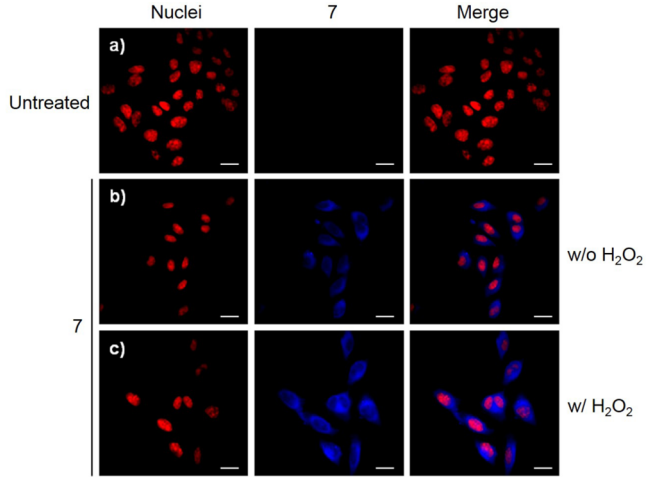

Figure 2. Cellular fluorescence images of prodrug 7-treated B16F10 cells. Cells were treated with 50 μM prodrug 7 for 6 h. Then, cells were treated with vehicle (b) or (c) H_2O_2 (100 μM) and incubated for 12 h. The nuclei of cells were stained by DRAQ5 (red). Scale bars: 20 μm. All images were acquired using these excitation wavelengths, 640/20 nm for nuclei and 360/40 nm for prodrug 7, and emission wavelengths, 685/15 nm for nuclei and 457/50 for prodrug 7.

HeLa cells were pretreated with prodrug 7 (50 μM) for 6 h, then exogenous H_2O_2 (100 μM) was added. After incubation for 12 h, fluorescence was visualized using a confocal fluorescence microscope. A weak fluorescence signal was observed in prodrug 7-treated cells in absence of endogenous H_2O_2 (Figure 2b and Supporting Information Figure S5b). Both cell types treated with exogenous H_2O_2 exhibited enhanced fluorescence (Figure 2c and Supporting Information Figure S5c). This result indicates that the oxidation of boronate moiety of prodrug 7 generated the fluorescence enhancement, depending upon amount of intracellular H_2O_2, as depicted in Scheme 2.

To provide further confirmation for H_2O_2-mediated cleavage of the boronate moiety and concomitant formation of fluorescent probe **8**, intracellular fluorescence was analyzed after exposure to phorbol 12-myristate 13-acetate (PMA). PMA is a stimulus for cytoplasmic NADPH oxidase and ROS generation.[17] The results shown in Supporting Information Figure S6 indicate that fluorescence in prodrug 7-treated B16F10 and HeLa cells was increased in the presence of PMA (0.5 μM).These data confirmed that the fluorescence enhancement of prodrug 7 was mainly induced by the overproduction of ROS like H_2O_2, and prodrug 7 could be used as a diagnostic agent for the detection of intracellular H_2O_2.

Previous studies reported that intracellular H_2O_2 was mainly produced by mitochondria and diffuses into lysosomes. A fluorescence probe can specifically detect intracellular H_2O_2 in

dx.doi.org/10.1021/ja5077684 | J. Am. Chem. Soc. 2014, 136, 13888−13894

the lysosomes.[7b,18] The lysosomal localization of activated prodrug 7 triggered by H_2O_2 was investigated using a selective fluorescent marker for lysosomes (LysoTracker-Red). As shown in Figure 3, fluorescence images of prodrug 7

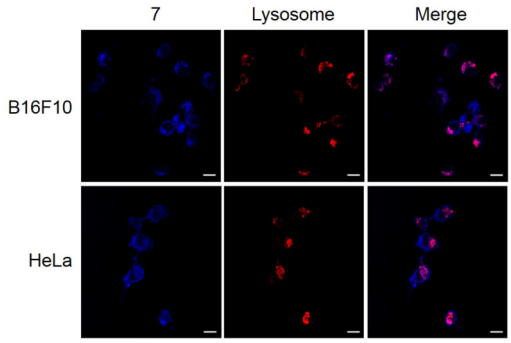

Figure 3. Subcellular localization of fluorescent prodrug 7 in B16F10 and HeLa cells. Cells were treated with 50 μM prodrug 7 for 6 h. Then, cells were treated with 100 μM H_2O_2 and further incubated for 12 h. LysoTracker-Red was used to identify the lysosomes. Images were collected with an excitation wavelengths at 555/28 nm and emission wavelenghts at 617/73 nm. (Scale bars: 20 μm).

overlapped with fluorescent images of lysosomes in B16F10 and HeLa cells. Therefore, H_2O_2-mediated cleavage of prodrug 7 occurred in the lysomes. This cleavage process inside the cells promotes the release of the fluorogenic coumarin moiety and concomitantly fluorescence activation. Together, these data indicate that prodrug 7 could be considered a specific marker for hydrogen peroxide in lysosomes.

The comparative anticancer effects of the prodrug 7 and SN-38 were assessed in B16F10 and HeLa cells by using a colorimetric cell viability assay. Both cells were treated with prodrug 7 or SN-38 at various concentrations (0−100 μM) for 6 h. This incubation was followed by addition of exogenous H_2O_2 to some of the prodrug 7-treated cells. After incubation for an additional 48 h, the methyl thiazole tetrazolium, (3-[4,5-dimethylthiazol-2-yl]-2,5-diphenyl tetrazolium bromide, MTT) assay was performed to determine cell viability. As shown in Figure 4, prodrug 7 showed concentration-dependent, antiproliferative effects against B16F10 and HeLa cells in the presence of H_2O_2. SN-38 cytotoxicity in both cells was identical to that of prodrug 7 at 100 μM. However, prodrug 7 showed less cytotoxicity under normal conditions (without H_2O_2), even at 100 μM. These results confirmed that the anticancer activity of prodrug 7 depends on H_2O_2, even though only H_2O_2 treatment slightly affected cell viability by H_2O_2-mediated apoptosis.[3d] Specific release and accumulation of SN-38 activated by H_2O_2 in cancer cells could prevent adverse effects of the direct SN-38 treatment.

Finally, we investigated the therapeutic potential of prodrug 7 in a metastatic lung tumor model to evaluate its anticancer efficacy *in vivo*. Metastatic tumors were induced by intravenous injection of B16F10 melanoma cells. Prodrug 7 (0.25 mg/kg) was administered intratracheally four times after tumor inoculation.[19] Noninvasive magnetic resonance imaging (MRI) was used for detecting tumor growth and therapeutic response.[20] As shown in Figure 5, the pulmonary tumors were noninvasively monitored using MRI on day 10. Discrete lung tumors were visualized in prodrug 7-treated mice, whereas diffuse metastatic tumors were observed in lung tissue of saline-treated mice.

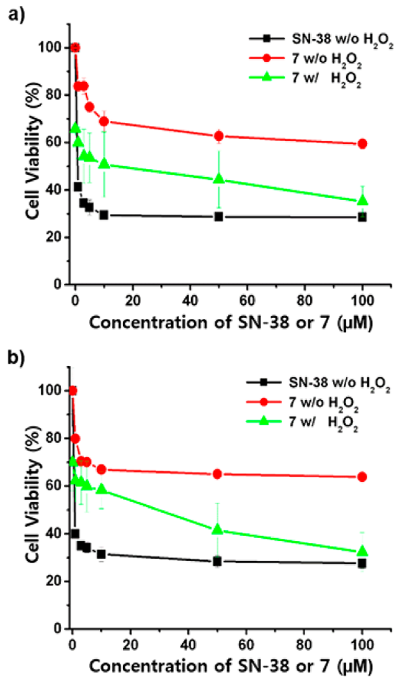

Figure 4. Antiproliferative activity of SN-38 and prodrug 7 in B16F10 (a) and HeLa (b) cell lines. Both cell lines were treated with SN-38 or prodrug 7 at various concentration (0−100 μM) for 6 h. After cells were treated with and without H_2O_2 (100 μM) for 48 h, cell viability was assessed by the methyl thiazole tetrazolium (MTT) assay.

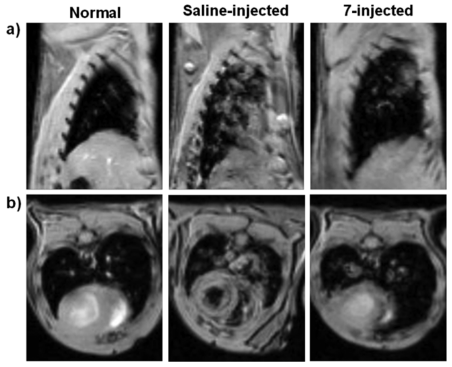

Figure 5. Representative *in vivo* magnetic resonance images of the mouse lungs in sagittal (a) and axial (b) planes. Mice with experimental lung metastasis induced by B16F10 melanomal cells were treated intratracheally with saline or prodrug 7. MRI scans were performed at day 10 postinoculation for monitoring the progression comparison of metastatic lung tumors.

The mice were sacrificed at day 17 and lung tissues were extracted for morphologic studies. While lung tissues of a saline-treated control group showed numerous black colonies of B16F10 cells, prodrug 7 inhibited tumor growth and likely preserved more normal lung tissue (Figure 6a). These observations were consistent with the histological findings observed with hematoxylin and eosin (H&E) staining (Figure 6b). These results were also supported by the prolonged survival time of prodrug 7-treated mice compared to the control group (Figure 6c). Taken together, these data showed that prodrug 7 exhibited strong anticancer effects through H_2O_2-mediated SN38 release in a metastatic lung tumor model. Prodrug 7 was developed as a tumor-targeted drug delivery

dx.doi.org/10.1021/ja5077684 | J. Am. Chem. Soc. 2014, 136, 13888−13894

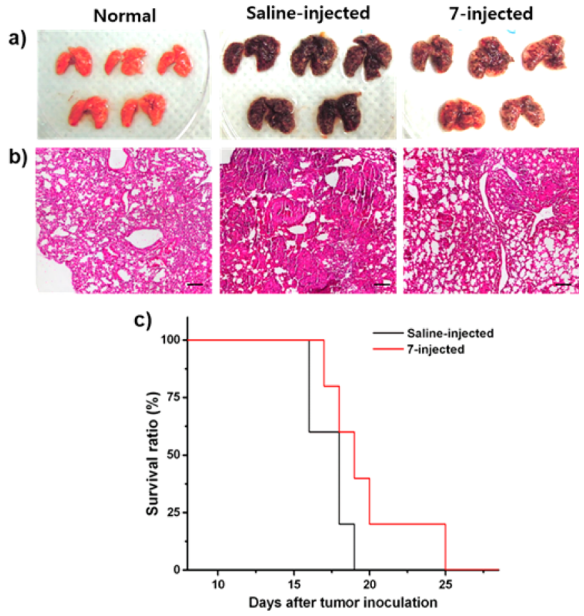

Figure 6. *In vivo* effects of prodrug **7** in an experimental lung metastasis model. (a) Representative lungs isolated from normal mice and mice with lung tumors administered saline or prodrug **7** intratracheally. (b) Histological sections of lung tissues with H&E staining. Scale bars: 100 μm. (c) Kaplan–Meier survival analysis of mice administered with saline or prodrug **7**.

system that can be specifically activated by ROS in the tumor environment.

CONCLUSIONS

In this study, a new theranostic prodrug **7** was developed, which contains a H_2O_2-induced cleavable boronate ester for activating a fluorescent moiety (coumarin) and releasing a potent anticancer drug, SN-38. Cellular H_2O_2 initiated disintegration of the prodrug **7** by the oxidation of aryl boronates to phenols, which produced the active SN-38 molecule and the free coumarin. Prodrug **7** showed a fluorescent signal localized inside the cell, especially in lysosomes, indicating the cellular delivery of the therapeutic agent, SN-38. This prodrug effectively inhibited cancer cell growth in the presence of H_2O_2 *in vitro*. In addition, *in vivo* therapeutic activity was demonstrated after intratracheal injection of prodrug **7** into mice with metastatic lung tumors. These studies confirmed that the prodrug selectively accumulated in metastasized lung tumors, where it released the active anticancer agent SN-38. Thus, prodrug **7** reacts with physiological levels of H_2O_2, resulting in dissociation of the conjugates and delivery of chemotherapeutic agent, providing a powerful new tool for cancer therapy.

EXPERIMENTAL SECTION

Synthesis of (*E*)-Ethyl 3-(7-hydroxy-2-oxo-2*H*-chromen-3-yl)acrylate (1). This compound was synthesized following the published procedure,[15] yield: 85%. ^{1}H NMR (DMSO-d_6, 300 MHz): δ 1.23 (t, J = 7.1 Hz, 3H), 4.15 (q, J = 7.1 Hz, 2H), 6.72 (d, J = 2.1 Hz, 1H), 6.80–6.85 (m, 2H), 7.45–7.55 (m, 2H), 8.40 (s, 1H). ^{13}C NMR (DMSO-d_6, 100 MHz): 14.8, 60.7, 102.5, 112.1, 114.6, 116.8, 120.3, 131.5, 139.5, 146.1, 156.0, 159.8, 163.5, 166.9 ppm.

Synthesis of (*E*)-Ethyl 3-(7-acetoxy-2-oxo-2*H*-chromen-3-yl)acrylate (2). This compound was synthesized following the published procedure,[15] yield: 88%. ^{1}H NMR (DMSO-d_6, 400 MHz): δ 1.05 (t, J = 7.1 Hz, 3H), 2.11 (s, 3H), 3.99 (q, J = 7.1 Hz, 2H), 6.73 (d, J = 16.0 Hz, 1H), 7.00 (dd, J = 2.1, 8.4 Hz, 1H), 7.12 (d, J = 2.0 Hz, 1H), 7.33 (d, J = 16.0 Hz, 1H), 7.56 (d, J = 8.5 Hz, 1H), 8.35 (s, 1H). ^{13}C NMR (DMSO-d_6, 100 MHz): 14.8, 21.5, 60.9, 110.67, 119.9, 121.1, 122.4, 130.8, 138.8, 144.9, 154.3, 154.5, 159.3, 166.6, 169.4 ppm.

Synthesis of 3-Formyl-2-oxo-2*H*-chromen-7-yl Acetate (3). This compound was synthesized following the published procedure[15] yield: 65%. ^{1}H NMR (DMSO-d_6, 400 MHz): δ 2.29 (s, 3H), 7.21–7.24 (m, 1H), 7.35 (d, J = 1.6 Hz, 1H), 8.00 (d, J = 8.6 Hz, 1H), 8.66 (s, 1H), 9.99 (s, 1H). ^{13}C NMR (DMSO-d_6, 100 MHz): 21.6, 111.0, 116.8, 120.2, 121.7, 133.1, 146.9, 156.0, 156.3, 159.7, 169.3, 188.7 ppm.

Synthesis of 7-Hydroxy-2-oxo-2*H*-chromene-3-carbaldehyde (4). Compound **3** (500 mg, 2.15 mmol) was dissolved in 40 mL of MeOH. K_2CO_3 (595 mg, 4.31 mmol) was added and the solution was stirred at room temperature for 30 min. After completion of the reaction (determined by TLC), the reaction mixture was acidified with 1 N HCl solution (pH 3–4), then filtered, washed twice with water, and dried. The crude yellow product **4** was pure enough for further step. Yield was 88%. ^{1}H NMR (DMSO-d_6, 400 MHz): δ 6.73–6.74 (m, 1H), 6.83 (d, J = 8.6 Hz, 1H), 7.78 (d, J = 8.7 Hz, 1H), 8.55 (s, 1H), 9.92 (s, 1H). ^{13}C NMR (DMSO-d_6, 100 MHz): 102.9, 111.6, 115.2, 117.8, 134.1, 147.9, 158.2, 160.4, 165.5, 188.5 ppm.

Synthesis of 3-Formyl-2-oxo-2*H*-chromen-7-yl Trifluoromethanesulfonate (5). Compound **4** (100 mg, 0.52 mmol) and pyridine (0.06 mL, 0.73 mmol) were dissolved in 20 mL of dichloromethane and stirred in an ice bath for 10 min. Trifluoromethanesulfonic anhydride (106 μL, 0.63 mmol) was slowly added. The reaction mixture was stirred for 2 h. After completion of the reaction (determined by TLC), the reaction mixture was diluted with dichloromethane (DCM), washed twice with brine, dried over sodium sulfate, then filtered, and the solvent was removed under reduced pressure. The crude product was purified by column chromatography on silica gel (EtOAc/hexane 1:9 to 2:8) to give compound **5** (120 mg, 71% yield) as a white solid. ^{1}H NMR ($CDCl_3$, 300 MHz): δ 7.24–7.31 (m, 1H), 7.34 (d, J = 2.0 Hz, 1H), 7.80 (d, J = 8.6 Hz, 1H), 8.40 (s, 1H), 10.23 (s, 1H). ^{13}C NMR ($CDCl_3$, 100 MHz): 111.0, 118.2, 118.9, 122.5, 132.7, 132.8, 144.3, 153.0, 156.2, 159.0, 187.3 ppm. HRMS: calculated for $C_{11}H_6F_3O_6S$ (M + 1) 322.9837; found 322.9836.

Synthesis of 3-(Hydroxymethyl)-7-(4,4,5,5-tetramethyl-1,3,2-dioxaborolan-2-yl)-2*H*-chromen-2-one (6). Compound **5** (100 mg, 0.31 mmol) was added to a stirred solution of bis(pinacolato)diboron (95 mg, 0.37 mmol), Pd(dppf)Cl_2·CH_2Cl_2 (12 mg, 0.01 mmol) and KOAc (91 mg, 0.93 mmol) in dry dioxane (5 mL). The reaction mixture was refluxed under an argon atmosphere for 8 h. After completion of the reaction (determined by TLC), the solvent was removed under reduced pressure. Then, the reaction mixture was diluted with EtOAc, washed twice with brine, dried over sodium sulfate, and filtered, and the solvent was removed under reduced pressure. The crude product was used for next step without further purification. This was done because the boronate linker in this compound is unstable in silica, even neutral alumina, or preparative TLC. The crude product (180 mg) was dissolved in 10 mL of MeOH and then $NaBH_4$ (38 mg, 1.02 mmol) was added. The reaction mixture was stirred at room temperature for 1 h. The reaction mixture was decomposed with saturated ammonium chloride solution and then diluted with EtOAc, washed twice with brine, dried over sodium sulfate, and filtered, and the solvent was removed under reduced pressure. The crude product was used for further steps without purification. The crude product **6** was analyzed using ^{1}H and ^{13}C NMR spectroscopy before going to the final step. ^{1}H NMR (300 MHz, $CDCl_3$): δ 1.36 (s, 12H), 4.63 (s, 2H), 7.46–7.49 (m, 1H), 7.68 (d, J = 7.4 Hz, 1H), 7.75 (d, J = 8.1 Hz, 1H), 7.81 (s, 1H). ^{13}C NMR (100 MHz, $CDCl_3$): 24.4, 24.5, 60.9, 82.9, 119.8, 122.3, 122.8, 130.0, 130.4, 130.9, 145.9, 154.9, 160.4 ppm. HRMS: calculated for $C_{16}H_{19}BO_5$ (M + Na) 325.1223, found 325.1227.

Synthesis of 7. To a stirred solution of **6** (70 mg, 0.23 mmol) and DIPEA (149 mg, 1.15 mmol, 0.20 mL) in dry dichloromethane (5.0 mL) was added phosgene solution (68 mg, 0.69 mmol, 0.34 mL). The reaction mixture was stirred at 0 °C under an argon atmosphere. After

dx.doi.org/10.1021/ja5077684 | J. Am. Chem. Soc. 2014, 136, 13888–13894

2 h, the excess phosgene was removed from the reaction mixture by an argon purge. Then the drug SN-38 (15 mg, 0.38 mmol in dry dichloromethane with few drops of dry DMF) was added to the reaction mixture and kept stirring for 5 days. After completion of the reaction (determined by TLC), the reaction mixture was diluted with EtOAc, washed twice with brine, dried over sodium sulfate, and filtered, and the solvent was removed under reduced pressure. The crude product was rapidly purified by short length column chromatography on neutral alumina (MeOH/DCM 1:9 to 3:7) and triturated with diethyl ether to give **7** (5.0 mg, 18.2% yield) as brownish solid. ^{1}H NMR (400 MHz, DMSO-d6): δ 0.88.00 (t, J = 7.2 Hz, 3H), 1.22 (t, J = 7.2 Hz, 3H), 1.32 (s, 12H), 1.97 (m, 2H), 3.09 (m, 2H), 3.50 (m, 2H), 5.17 (s, 2H), 5,42 (s, 2H) 6.49 (s, 1H), 7.25 (s, 1H), 7.40−7.757 (m, 3H), 8.03 (d, J = 8.32 Hz, 2H). ^{13}C NMR (100 MHz, $CDCl_3$ with two drops DMSO-d_6): 8.2, 13.8, 22.7, 25.1, 25.4, 29.4, 30.6, 49.9, 65.7, 70.2, 72.8, 96.2, 105.2, 118.4,122.8, 128.4, 128.6, 132.0, 143.2, 144.1, 146.9, 149.3, 150.5, 157.2,157.3, 173.0 ppm. HRMS: calculated for $C_{39}H_{37}BN_2O_{11}$ (M + H) 721.2467, found 721.2426.

Synthesis of 7-Hydroxy-3-(hydroxymethyl)-2*H*-chromen-2-one (8). To a stirred solution of **4** (80 mg, 0.42 mmol) in methanol (5.0 mL) was added sodium borohydride (26 mg, 0.72 mmol). The reaction mixture was stirred at room temperature for 2 h. After completion of the reaction (determined by TLC), the reaction mixture was decomposed with ammonium chloride solution, diluted with EtOAc, washed twice with brine, dried over sodium sulfate, and filtered, and the solvent was removed under reduced pressure. The crude product was purified by column chromatography on silica gel (MeOH/DCM 0.5:9.5 to 1:9) to give **8** (35 mg, 44% yield) as a very light yellow solid. ^{1}H NMR (300 MHz, $CDCl_3$): δ 4.51 (s, 2H), 6.77−6.81 (m, 2H), 7.32 (d, J = 8.5 Hz, 1H), 7.75 (s, 1H) ppm. HRMS: calculated for $C_{10}H_8O_4$ (M + 1) 193.0501; found 193.0501.

Synthetic Materials and Methods. Chemicals used in this project were purchased from Aldrich, Alfa-Aesar, Carbosynth, TCI, and Ducsan without further purification. Silica gel 60 (Merck, 0.063-0.2 mm) was used for column chromatography. Analytical TLC was performed using Merck 60 F254 silica gel (precoated sheets, 0.25 mm thick). ^{1}H and ^{13}C NMR spectra were collected in $CDCl_3$, DMSO (Cambridge Isotope Laboratories, Cambridge, MA) on Varian 300 and 400 MHz spectrometers. All chemical shifts are reported in ppm values using the peak of residual proton signals of TMS as an internal reference. The mass spectra were obtained on an Ion Spec Hi-Res mass spectrometer.

Spectroscopic Materials and Methods. Different reactive oxygen species (ROS) were used to treat prodrug **7** as follows: 5 mM superoxide (O_2^-) and 100 μM of all other ROS. Superoxide used as solid KO_2. Hydrogen peroxide (H_2O_2), *tert*-butyl hydroperoxide (TBHP), and hypochlorite ion (OCl^-) were used as commercially available 30%, 70%, and 5% aqueous solutions. The *tert*-butoxy radical ($\cdot O^tBu$) and hydroxyl radical ($\cdot OH$) were prepared by the reaction of Fe^{2+} (1 mM) with TBHP (100 μM), or H_2O_2 (100 μM), respectively. Stock solutions of prodrug **7** were prepared in triple 3′ distilled water. All spectroscopic measurements were performed under physiologic conditions (PBS buffer containing 10% (v/v) DMSO, pH 7.4, 37 °C). Absorption spectra were recorded on an S-3100 (Scinco) spectrophotometer, and fluorescence spectra were recorded using an RF-5301 PC spectrofluorometer (Shimadzu) equipped with a xenon lamp. Samples for absorption and emission measurements were contained in quartz cuvettes (3 mL volume). Excitation was provided at 320 nm with excitation and emission slit widths of 3 nm.

Preparation of Cell Cultures and Fluorescence Imaging. The mouse melanoma cells (B16F10), and human cervical cancer (HeLa) cells were grown at 37 °C in an atmosphere of 5% CO_2 using Dulbecco's Modified Eagle's Medium supplemented with 10% fetal bovine serum and an antibiotic−antimycotic mixture (Invitrogen-Gibco, Carlsbad, CA). The cellular uptake of prodrug **7** was confirmed by fluorescence microscopy. B16F10 and HeLa cells were seeded in an 8-well slide (Ibidi, Munich, Germany), and grown to a density of 25 000 cells per well. All cells were incubated with 50 μM prodrug **7** in media for 6 h, and then 0.1 mM H_2O_2 was added.

To induce the intracellular H_2O_2 production, both cells types were treated with 20 μM prodrug **7** and incubated with PMA (0.5 μg/mL). Cells were washed with phosphate-buffered saline (PBS) for three times after incubation for 12 h. Fluorescent images were taken with a Deltavision microscope (Applied Precision, Issaquah, WA). Nuclei were counterstained with DRAQ-5 (Biostatus Limited, U.K.) for 20 min at room temperature. LysoTracker Red (Invitrogen, Grand Island, NY) was used to investigate the colocalization of prodrug **7** with lysosomes. Cell images were obtained by an LSM 410 confocal microscope (Carl Zeiss Inc., Germany).

Cell Viability Assay. Antiproliferative activity of prodrug **7** and SN-38 was tested by the MTT assay. Cells were seeded into 96-well culture plates at 5 × 10^3 cells/well and incubated for 24 h at 37 °C. Each compound was added to the wells at concentrations ranging from 1 to 100 μM for 6 h, and then the cells were cultured for 48 h after addition of 0.1 mM H_2O_2. As a control, both cell types were incubated without H_2O_2 treatment. The MTT assay was performed using a commercially available MTT assay kit (Roche Diagnostics, Mannheim, Germany) according to manufacturer's instructions. In brief, MTT labeling reagent was added to wells and incubated for 3 h at 37 °C, followed by an overnight incubation with the solubilization buffer. Finally, the absorbance of each well was measured at 570 nm using a microplate reader (VersaMax, Molecular Devices, Sunnyvale, CA).

***In Vivo* Antitumor Efficacy in a Mouse Metastatic Lung Tumor Model.** To determine whether prodrug **7** has therapeutic potential in the treatment of metastatic cancer, mice were injected intravenously with 0.1 mL of cell suspension containing 1 × 10^6 B16F10 melanoma cells to generate metastatic lung tumors. After 3 days, prodrug **7** (250 μg/kg) was intratracheally delivered to the lung tissues four times every 2 days, using a microsprayer (Penn-Century, Inc., Glenside, PA). The progression of metastasized lung tumors was noninvasively monitored at day 10, using a 4.7 T animal MRI scanner (Biospec 47/40, Bruker, Germany) with gradient-echo pulse sequence (TE/TR = 4.2/247 ms, slice thickness = 1 mm, FOV = 3 × 3 cm^2, matrix = 128 × 128, NEX = 8). The antitumor effect of prodrug **7** was determined by morphological and histological examination of lung tissues. After weighing each mouse, the mice (n = 5 each for mice treated with saline and prodrug **7**) were sacrificed on day 17, followed by collection of lung tissues and microscopic examination of tissue section slides using H&E staining (TissueGnostics GmbH, Vienna, Austria). Survival rates of control and experimental group (n = 10 each) were determined using a Kaplan−Meier survival analysis.

■ ASSOCIATED CONTENT

Ⓢ Supporting Information

Experimental details including syntheses, characterization data (^{1}H NMR, ^{13}C NMR, mass spectra), and figures (fluorescence cell images). This material is available free of charge via the Internet at http://pubs.acs.org.

■ AUTHOR INFORMATION

Corresponding Authors

jongskim@korea.ac.kr
kshong@kbsi.re.kr
sukhen_chem@yahoo.com

Present Address

‖Amrita Centre for Industrial Research & Innovation, Amrita University, Ettimadai, Coimbatore, India 641 112.

Notes

The authors declare no competing financial interest.

■ ACKNOWLEDGMENTS

This work was supported by the Creative Research Initiative program (No. 2009-0081566) of National Research Foundation of Korea, the CAP (PBD066) funded by the Korea Research Council of Fundamental Science and Technology,

and by a grant from the Korea Basic Science Institute (D34400).

REFERENCES

(1) (a) Chambers, A. F.; Groom, A. C.; MacDonald, I. C. *Nat. Rev. Cancer* **2002**, *2*, 563−572. (b) Lotfi-Jam, K.; Carey, M.; Jefford, M.; Schofield, P.; Charleson, C.; Aranda, S. *J. Clin. Oncol.* **2008**, *26*, 5618−5629. (c) Goss, P. E.; Chambers, A. F. *Nat. Rev. Cancer* **2010**, *10*, 871−877. (d) Lammers, T.; Kiessling, F.; Hennink, W. E.; Storm, G. *J. Controlled Release* **2012**, *161*, 175−187.

(2) (a) Szatrowski, T. P.; Nathan, C. F. *Cancer Res.* **1991**, *51*, 794−798. (b) Zieba, M.; Suwalski, M.; Kwiatkowska, S.; Piasecka, G.; Grzelewska-Rzymowska, I.; Stolarek, R.; Nowak, D. *Respir. Med.* **2000**, *94*, 800−805. (c) Lim, S. D.; Sun, C.; Lambeth, J. D.; Marshall, F.; Amin, M.; Chung, L.; Petros, J. A.; Arnold, R. S. *Prostate* **2005**, *62*, 200−207. (d) Schumacker, P. T. *Cancer Cell* **2006**, *10*, 175−176. (e) Trachootham, D.; Alexandre, J.; Huang, P. *Nat. Rev. Drug Discovery* **2009**, *8*, 579−591.

(3) (a) Oktyabrsky, O.; Smirnova, G. *Biochemistry (Moscow)* **2007**, *72*, 132−145. (b) López-Lázaro, M. *Cancer Lett.* **2007**, *252*, 1−8. (c) Reuter, S.; Gupta, S. C.; Chaturvedi, M. M.; Aggarwal, B. B. *Free Radical Biol. Med.* **2010**, *49*, 1603−1616. (d) Fang, J.; Nakamura, H.; Iyer, A. K. *J. Drug. Target* **2007**, *15*, 475−486.

(4) (a) Ishikawa, K.; Takenaga, K.; Akimoto, M.; Koshikawa, N.; Yamaguchi, A.; Imanishi, H.; Nakada, K.; Honma, Y.; Hayashi, J. *Science* **2008**, *320*, 661−664. (b) Pani, G.; Galeotti, T.; Chiarugi, P. *Cancer Metastasis Rev.* **2010**, *29*, 351−378.

(5) (a) Hempel, N.; Ye, H.; Abessi, B.; Mian, B.; Melendez, J. A. *Free Radical Biol. Med.* **2009**, *46*, 42−50. (b) Hempel, N.; Bartling, T. R.; Mian, B.; Melendez, J. A. *Mol. Cancer Res.* **2013**, *11*, 303−312.

(6) (a) Lippert, A. R.; Van de Bittner, G. C.; Chang, C. J. *Acc. Chem. Res.* **2011**, *44*, 793−804. (b) Zhou, J.; Tsai, Y.-T.; Weng, H.; Tang, L. *Free Radical Biol. Med.* **2012**, *52*, 218−226. (c) Lee, S. H.; Gupta, M. K.; Bang, J. B.; Bae, H.; Sung, H. J. *Adv. Healthcare Mater.* **2013**, *2*, 908−915. (d) Lallana, E.; Tirelli, N. *Macromol. Chem. Phys.* **2013**, *214*, 143−158.

(7) (a) Miller, E. W.; Tulyathan, O.; Isacoff, E. Y.; Chang, C. J. *Nat. Chem. Biol.* **2007**, *3*, 263−267. (b) Song, D.; Lim, J. M.; Cho, S.; Park, S. J.; Cho, J.; Kang, D.; Rhee, S. G.; You, Y.; Nam, W. *Chem. Commun.* **2012**, *48*, 5449−5451. (c) Oh, W. K.; Jeong, Y. S.; Kim, S.; Jang, J. *ACS Nano* **2012**, *6*, 8516−8524. (d) Weinstain, R.; Savariar, E. N.; Felsen, C. N.; Tsien, R. Y. *J. Am. Chem. Soc.* **2014**, *136*, 874−877.

(8) Chen, X.; Pradhan, T.; Wang, F.; Kim, J. S.; Yoon, J. *Chem. Rev.* **2012**, *112*, 1910−1956.

(9) (a) Jokerst, J. V.; Gambhir, S. S. *Acc. Chem. Res.* **2011**, *44*, 1050−1060. (b) Akhter, S.; Ahmad, I.; Ahmad, M. Z.; Ramazani, F.; Singh, A.; Rahman, Z.; Ahmad, F. J.; Storm, G.; Kok, R. J. *Curr. Cancer Drug Targets* **2013**, *13*, 362−378. (c) Kim, T. H.; Lee, S.; Chen, X. *Expert Rev. Mol. Diagn.* **2013**, *13*, 257−269. (d) Bao, G.; Mitragotri, S.; Tong, S. *Annu. Rev. Biomed. Eng.* **2013**, *15*, 253−282.

(10) (a) Lee, M. H.; Kim, J. Y.; Han, J. H.; Bhuniya, S.; Sessler, J. L.; Kang, C.; Kim, J. S. *J. Am. Chem. Soc.* **2012**, *134*, 12668−12674. (b) Maiti, S.; Park, N.; Han, J. H.; Jeon, H. M.; Lee, J. H.; Bhuniya, S.; Kang, C.; Kim, J. S. *J. Am. Chem. Soc.* **2013**, *135*, 4567−4572. (c) Bhuniya, S.; Lee, M. H.; Jeon, J. H.; Han, J. H.; Lee, J. H.; Park, N.; Maiti, S.; Kang, C.; Kim, J. S. *Chem. Commun.* **2013**, *49*, 7141−7143. (d) Bhuniya, S.; Maiti, S.; Kim, E. J.; Lee, H.; Sessler, J. L.; Hong, K. S.; Kim, J. S. *Angew. Chem., Int. Ed.* **2014**, *53*, 4469−4474.

(11) (a) Miller, E. W.; Albers, A. E.; Pralle, A.; Isacoff, E. Y.; Chang, C. J. *J. Am. Chem. Soc.* **2005**, *127*, 16652−16659. (b) Dickinson, B. C.; Chang, C. J. A. *J. Am. Chem. Soc.* **2008**, *130*, 9638−9639. (c) Miller, E. W.; Tulyathan, O.; Isacoff, E. Y.; Chang, C. J. *Nat. Chem. Biol.* **2007**, *3*, 263−267.

(12) (a) Kuivila, H. G.; Armour, A. G. *J. Am. Chem. Soc.* **1957**, *79*, 5659−5662. (b) Yang, W. Q.; Gao, X.; Wang, B. H. In *Boronic Acids*; Hall, D. G., Ed.; Wiley-VCH: Weinheim, 2005; pp 481−512. (c) Lippert, A. R.; Van de Bittner, G. C.; Chang, C. J. *Acc. Chem. Res.* **2011**, *44*, 793−804.

(13) (a) Kuang, Y.; Balakrishnan, K.; Gandhi, V.; Peng, X. *J. Am. Chem. Soc.* **2011**, *133*, 19278−19281. (b) Liu, J.; Pang, Y.; Zhu, Z.; Wang, D.; Li, C.; Huang, W.; Zhu, X.; Yan, D. *Biomacromolecules* **2013**, *14*, 1627−1636.

(14) (a) Gatto, B.; Capranico, G.; Palumbo, M. *Curr. Pharm. Des.* **1999**, *5*, 195−215. (b) Mathijssen, R. H. J.; van Alphen, R. J.; Verweij, J.; Loos, W. J.; Nooter, K.; Stoter, G.; Sparreboom, A. *Clin. Cancer Res.* **2001**, *7*, 2182−2194.

(15) Lim, N. C.; Schuster, J. V.; Porto, M. C.; Tanudra, M. A.; Yao, L.; Freake, H. C.; Brückner, C. *Inorg. Chem.* **2005**, *44*, 2018−2030.

(16) Wang, M.; Qi, P.; Wu, D. *Drug Dev. Ind. Pharm.* **2003**, *29*, 661−667.

(17) Larsen, E. C.; DiGennaro, J. A.; Saito, N.; Mehta, S.; Loegering, D. J.; Mazurkiewicz, J. E.; Lennartz, M. R. *J. Immunol.* **2000**, *165*, 2809−2817.

(18) Kurz, T.; Terman, A.; Gustafsson, B.; Brunk, U. T. *Biochim. Biophys. Acta* **2008**, *1780*, 1291−1303.

(19) Shim, G.; Choi, H. W.; Lee, S.; Choi, J.; Yu, Y. H.; Park, D. E.; Choi, Y.; Kim, C. W.; Oh, Y. K. *Mol. Ther.* **2013**, *21*, 816−824.

(20) (a) Tidwell, V. K.; Garbow, J. R.; Krupnick, A. S.; Engelbach, J. A.; Nehorai, A. *Magn. Reson. Med.* **2012**, *67*, 572−579. (b) McCormack, E.; Silden, E.; West, R. M.; Pavlin, T.; Micklem, D. R.; Lorens, J. B.; Haug, B. E.; Cooper, M. E.; Gjertsen, B. T. *Cancer Res.* **2013**, *73*, 1276−1286.